Theoretical Analysis of Performance Characteristics of Non- Road Spark Ignition Engines

Abstract

Non-road spark ignition (SI) engines play a critical role in Nigeria, particularly in agriculture, construction, and small-scale power generation. Despite their extensive use, there is limited research on how Nigeria's unique environmental and operational conditions such as high ambient temperatures, poor fuel quality, and irregular maintenance practices affect the performance of these engines. This study presents a theoretical analysis of the performance characteristics of non-road SI engines under Nigerian conditions, focusing on fuel efficiency, power output, thermal efficiency, and emissions. The effect of engine speed, engine load and equivalence ratio on the performance characteristics of non-road spark ignition engines were studied in this research. Three operating parameters (engine load, engine speed, and equivalence ratio) and eight engine performance parameters which are Brake Specific Fuel Consumption (BSFC), Brake Power (BP), Thermal Efficiency (TE), Brake Mean Effective Pressure, Exhaust Gas Temperature (EGT), carbon monoxide emission, hydrocarbon emission, and nitrogen oxide were considered in this work. Theoretical analysis was performed using a two-zone SI engine model, the resulting equations were solved with the aid of a computer program developed by the authors and implemented in MATLAB software. The effect of the operating parameters on the performance parameters was simulated using the computer code developed which was implemented in MATLAB. The results show that the engine speed of 3000 rpm gave the optimum values of 250 g/kWh, 33 kW, 1070 kPa, 28% and 720 ^{o}C for BSFC, BP, BMEP, TE, and EGT respectively. Also, all performance parameters increased with an increase in engine load. The equivalence ratio of 0.9 gave the optimum values for all the parameters considered in this work. It can be concluded that for optimum performance of non-road SI engines, it should be operated at equivalence ratio of 0.9, engine speed of 3000 rpm and low engine loads.

Keywords: Performance Parameters, Exhaust Gas Emissions, Non-road SI Engines, and Equivalence Ratio.

1. INTRODUCTION

Non-road spark ignition (SI) engines are essential in various sectors of the Nigerian economy, playing a pivotal role in agriculture, construction, power generation, and transportation. In rural and semi-urban areas, where access to electricity is often limited, non-road SI engines are frequently used in irrigation pumps, small-scale generators, and other

machinery to power critical activities [1,2]. Despite their widespread use, the performance characteristics of these engines, including their fuel efficiency, durability, and emissions, remain under-researched, especially in the context of Nigeria's unique operational and environmental conditions. Nigeria's economy is heavily reliant on non-road SI engines, particularly in sectors such as agriculture and small-scale manufacturing. The agricultural sector, which accounts for approximately 24% of the nation's Gross Domestic Product (GDP) and employs over 70% of the population, depends on mechanized tools powered by SI engines for land preparation, irrigation, and post-harvest processing. Additionally, in remote areas where electricity infrastructure is underdeveloped, small SI engines provide essential energy for domestic and commercial applications, including powering homes, workshops, and small businesses [1,2.3].

The operating environment in Nigeria, characterized by high temperatures (usually over 35^{o}C), humidity, and dusty conditions, can have significant effects on the performance and longevity of these engines. Fuel quality is also a concern, as adulteration of gasoline and irregular supply often lead to suboptimal engine performance and higher emissions [4,5,6]. Therefore, understanding the theoretical aspects of how non-road SI engines perform under these conditions is critical for optimizing their operation in the country. Non-road SI engines in Nigeria face unique challenges that impact their performance. These engines often operate under severe conditions, including high ambient temperatures, which can affect combustion efficiency and reduce overall engine lifespan. Poor fuel quality due to impurity level and maintenance practices further exacerbate these issues, leading to reduced power output, increased fuel consumption, and higher levels of pollutant emissions [7,8,9]. However, these challenges present opportunities for innovation and improvement. By applying advanced thermodynamic models and combustion theory, it is possible to predict and optimize the performance of non-road SI engines, taking into account the specific conditions in Nigeria [2].

The environmental impact of non-road SI engines in Nigeria is significant, particularly in terms of air pollution. Nigeria is one of the largest consumers of gasoline-powered generators in sub-Saharan Africa, with millions of small engines contributing to local air quality deterioration, especially in densely populated urban areas. Emissions from these engines include harmful pollutants such as carbon monoxide (CO), unburned hydrocarbons (HC) and oxides of Nitrogen (NO_x), which are known to have adverse effects on human health and the environment. Regulatory frameworks to control emissions from non-road engines in Nigeria are less stringent compared to those in developed countries, where strict standards are enforced. The National

Environmental Standards and Regulations Enforcement Agency (NESREA) has introduced guidelines aimed at reducing emissions, but enforcement remains weak [10,11,12]. Moreover, the absence of localized emission testing for non-road SI engines means that there is limited data on their environmental impact. This study bridges this gap by providing a theoretical understanding of how these engines can be optimized to meet potential future emission standards.

This study applied theoretical modeling techniques to evaluate the performance characteristics of non-road SI engines in Nigeria. Thermodynamic cycle analysis was used to simulate the Otto cycle, which is commonly used to model spark ignition engines to create a more accurate representation of engine behaviour under Nigerian operating conditions [13,14,15]. The parameters to be studied include the equivalence ratio, engine speed, and engine load. By simulating these factors, the study provided insights into how non-road SI engines can be adapted to operate more efficiently and sustainably in Nigeria [16,17,18]. By providing a theoretical analysis of engine performance under local conditions, this research offered practical solutions for improving efficiency, reducing emissions, and ensuring the sustainability of non-road engine operations in the country [19,20,21]. The study addressed the need to optimize these engines for local applications, focusing on improving power output, fuel consumption, and reducing harmful emissions. Given the increasing global emphasis on sustainability, the findings from this study have the potential to inform policies and practices that enhance energy efficiency while mitigating environmental impacts in Nigeria.

2. Material and Methods

This study investigated the effect of varying three operating parameters on eight performance parameters of non-road SI engines.

2.1 Operating Parameters.

The parameters considered are:

(i) Engine load

(ii) Engine speed

(iii) Equivalence ratio

2.1.1 Engine Speed

The range of engine speed for an SI engine is usually between 1000 rpm to 5000 rpm (Heywood, 2018). In this study, 3000 rpm was used as the baseline and it was varied from 1000 rpm to 5000 rpm at five levels (Table 1).

2.1.2 Engine Load

The engine load was varied from zero loading condition (0% loading condition) to when the engine is fully loaded (100% loading condition) at five levels. 50 % loading condition was used as the baseline.

2.1.3 Equivalence Ratio

An equivalence ratio of 1.0 is usually set for SI engines (stoichiometric Air/Fuel ratio) Heywood, 2018). An equivalence ratio of 1.0 was used as the baseline in this work and it was varied from 0.8 to 1.2 at five levels. Table 1 shows the operating parameters and the levels at which they are used. Other parameters considered were kept constant at their baseline values: Ignition Timing (spark timing) = 30^{o} Before Top Death Center (BTDC), Compression Ratio=10 and Exhaust Gas Recirculation (EGR) = 0 %.

Table 1: Operating Parameters at Five Levels

S/N	Parameters	Levels				
		1	2	3	4	5
1.	Equivalence ratio	0.8	0.9	1.0	1.1	1.2
2.	Engine speed (rpm)	1000	2000	3000	4000	5000
3.	Engine load (% loading condition)	0	25	50	75	100

2.2 Performance Parameters.

The parameters considered are:

1. Specific fuel consumption (SFC)
2. Brake power (BP)
3. Brake mean effective pressure (BMEP)
4. Thermal efficiency (η_{th})
5. Exhaust gas temperature (T_{EG})
6. Unburned Hydrocarbon (HC) emission
7. Carbon monoxide (CO) emission
8. Oxides of Nitrogen (NO_X) emission

2.3 Two-zone Engine Model

The combustion chamber is divided into “burned” and “unburned” zones in a two-zone technique (Heywood 2018). The flame propagation is moving from burned toward unburned zone during combustion as shown in plate 1. The merit of using a two-zone combustion technique

is to achieve a more accurate result when compared with the zero-dimensional technique while having fast simulation time for many cycles simulation.

The main assumptions used in a two-zone combustion model in this research are:

- The intake and exhaust strokes are reversible adiabatic processes.
- The compression and expansion strokes models are based on the first law of thermodynamics (single-zone model).
- The cylinder pressure is considered uniform during each stroke.
- The combustion process model is based on the turbulent flame propagation theory combined with the first law of thermodynamics.
- The flame front shape is assumed to be spherical. However, the flame thickness (volume) is assumed small in comparison with burned and unburned zones.
- Each zone has a uniform composition and temperature during the combustion process
- The burned and unburned gases are taken to be ideal gases.

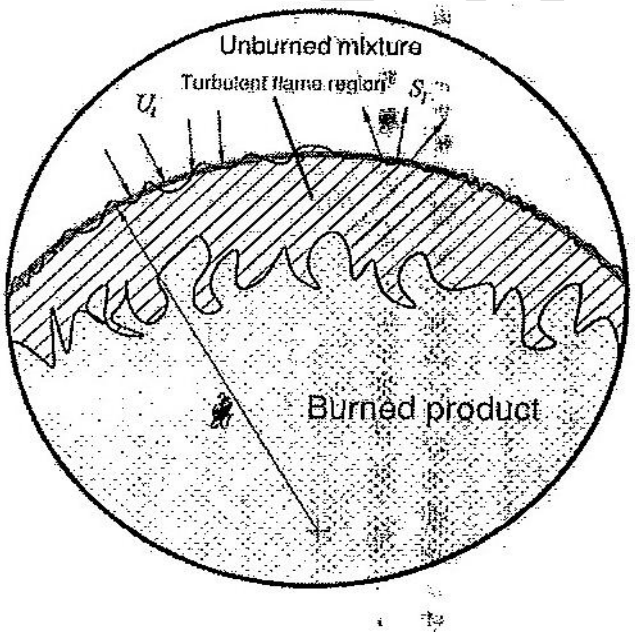

Plate 1: Schematic of Two-Zone Combustion Chamber

2.4 A-quasi-dimensional model equations

The basic equation for the engine model is derived from the conservation of energy applied to the cylinder volume:

$$dU = -\delta Q - \delta W + \sum_i h_i dm_i \quad (1)$$

Here,

U = the internal energy of the cylinder gas mixture

Q = heat exchange of the cylinder contents with the cylinder walls

W = work on the piston

h_i = specific enthalpy of in- or outflowing gas,

dm = mass flow into (+) or out of (-) the cylinder.

The work δW can be expressed as pdV,

Where p is the pressure and V is the cylinder volume.

2.4.1 Compression and expansion processes

Starting from conservation of energy,

$$\frac{d(mu)}{d\theta} = -\frac{dQ}{d\theta} - p\frac{dV}{d\theta} + h\frac{dm}{d\theta} \quad (2)$$

The left-hand side (LHS) can be rewritten as:

$$m\frac{du}{d\theta} + u\frac{dm}{d\theta} \quad (3)$$

$Note\ that\ du/d\theta = \partial u/\partial T.\, dT/d\theta = c_v dT/d\theta.\ h = u + RT$, where R is the gas constant of the mixture for an ideal gas.

Hence, the equation for the temperature change can be written as:

$$\frac{dT}{d\theta} = \frac{1}{mc_v}\left[\frac{dQ}{d\theta} - p\frac{dV}{d\theta} + \frac{dm}{d\theta}RT\right] \quad (4)$$

$with\ dm/d\theta\ resulting\ from\ blowby: dm/d\theta = dm_l/d\theta.$

The ideal gas equation $pV = mRT$ is differentiated for the pressure change

$$V\frac{dp}{d\theta} + p\frac{dV}{d\theta} = RT\frac{dm}{d\theta} + mT\ \frac{dR}{d\theta} + mR\frac{dT}{d\theta} \quad (5)$$

For compression stroke, the cylinder gas composition is taken to be constant and for expansion stroke, it is being taken to change only slowly, or $dR/d\theta \approx 0$,

Hence the equation for the pressure change becomes:

$$\frac{dp}{d\theta} = \frac{1}{V}\left(\frac{dm_l}{d\theta}RT + mR\ \frac{dT}{d\theta} - p\frac{dV}{d\theta}\right) \quad (6)$$

2.4.2 Combustion Process

Application of conservation of energy equation to the unburned gas zone results in the following equation:

$$\frac{d\, m_u u_u}{d\theta} = -\frac{dQ_u}{d\theta} - p\frac{dV_u}{d\theta} - h_u\frac{dm_x}{d\theta} - h_u\frac{dm_{l,u}}{d\theta} \quad (7)$$

Q_u = the heat exchange between the unburned zone and the cylinder walls,

V_u = the volume of the unburned zone,

$dm_x/d\theta$ = the mass burning rate (dm_x/dt)

$dm_{l,u}/d\theta$ = the leakage of unburned gas from the cylinder to the crankcase

LHS equation can be written as:

$$m_u\frac{du_u}{d\theta} + u_u\frac{dm_u}{d\theta} \quad (8)$$

$Note\ that\ \ du_u/d\theta = c_{v,u}dT_u/d\theta.$

The rate of change in the unburned gas can be written as:

$$\frac{dm_u}{d\theta} = -\frac{dm_x}{d\theta} - \frac{dm_{l,u}}{d\theta} \quad (9)$$

Resulting in:

$$m_u C_{v,u}\frac{dT_u}{d\theta} - \ u_u\frac{dm_x}{d\theta} = -\frac{dQ_u}{d\theta} - p\frac{dV_u}{d\theta} - h_u\frac{dm_x}{d\theta} - R_u T_u\frac{dm_{l,u}}{d\theta} \quad (10)$$

Application of conservation of energy equation for the burned gas zone results in:

$$\frac{d\, m_b u_b}{d\theta} = -\frac{dQ_b}{d\theta} - p\frac{dV_b}{d\theta} - h_u\frac{dm_x}{d\theta} - h_b\frac{dm_{l,b}}{d\theta} \quad (11)$$

Again,

$$\frac{d\, m_b u_b}{d\theta} = m_b\frac{du_b}{d\theta} + u_b\frac{dm_b}{d\theta} \quad (12)$$

$With\ du_b/d\theta = c_{v,b}dT_b/d\theta.$

The equation for the rate of change in the burned mass can be written as:

$$\frac{dm_b}{d\theta} = -\frac{dm_x}{d\theta} - \frac{dm_{l,b}}{d\theta} \quad (13)$$

Resulting in:

$$m_b C_{v,b}\frac{dT_b}{d\theta} + h_b\frac{dm_x}{d\theta} \ = \ -\frac{dQ_b}{d\theta} - p\frac{dV_b}{d\theta} + h_u\frac{dm_x}{d\theta} - R_b T_b\frac{dm_{l,b}}{d\theta} \quad (14)$$

The equation for the total internal energy balance can be written out, as the sum of the balances eq. (10) and (14)

$$m_u C_{v,u}\frac{dT_u}{d\theta} + m_b C_{v,b}\frac{dT_b}{d\theta} + U_b - \ U_u\ \frac{dm_x}{d\theta} \ =$$
$$-\frac{dQ}{d\theta} - p\frac{dV}{d\theta} - R_u T_u\frac{dM_{iu}}{d\theta} - R_b T_b\frac{dm_{l,b}}{d\theta} \quad (15)$$

Using

$$\frac{dV}{d\theta} = \frac{dV_u}{d\theta} + \frac{dV_b}{d\theta} \tag{16}$$

$$\frac{dQ}{d\theta} = \frac{dQ_u}{d\theta} + \frac{dQ_b}{d\theta} \tag{17}$$

The ideal gas equation for the two zones is differentiated to give:

$$p\frac{dV_u}{d\theta} + V_u\frac{dp}{d\theta} = R_u T_u \frac{dm_u}{d\theta} + m_u R_u \frac{dT_u}{d\theta} \tag{18}$$

$$p\frac{dV_b}{d\theta} + V_b\frac{dp}{d\theta} = R_b T_b \frac{dm_b}{d\theta} + m_b R_b \frac{dT_b}{d\theta} \tag{19}$$

Substituting Eq. (18) in Eq. (10) to get:

$$m_u C_{v,u}\frac{dT_u}{d\theta} - h_u - R_u T_u \frac{dm_x}{d\theta} = -\frac{dQ_u}{d\theta} - V_u\frac{dp}{d\theta}$$

$$-R_u T_u \frac{dm_u}{d\theta} - m_u R_u \frac{dT_u}{d\theta} - h_u \frac{dm_x}{d\theta} - R_u T_u \frac{dm_{l,u}}{d\theta} \tag{20}$$

Using $C_{v,u} + R_u = C_{p,u}$ and Eq. (9),

The rate of change of the unburned gas temperature equation is obtained:

$$\frac{dT_u}{d\theta} = \frac{1}{m_u C_{p,u}}\left(V_u\frac{dp}{d\theta} - \frac{dQ_u}{d\theta}\right) \tag{21}$$

Now, substituting $dV_u/d\theta$ and $dV_b/d\theta$ in Eq. (16) using equations. (18) and (19), gives:

$$\frac{dV}{d\theta} = \frac{R_u T_u}{P}\frac{dm_u}{d\theta} + \frac{m_u R_u}{P}\frac{dT_u}{d\theta} - \frac{V_u}{P}\frac{dp}{d\theta} + \frac{R_b T_b}{P}\frac{dm_b}{d\theta} + \frac{m_b R_b}{P}\frac{dT_b}{d\theta} - \frac{V_b}{P}\frac{dp}{d\theta} \tag{22}$$

Applying the ideal gas equation and equations (9) and (13) then, eq. 22 can be rewritten as:

$$\frac{dV}{d\theta} = \left(\frac{V_b}{m_b} - \frac{V_u}{m_u}\right)\frac{dm_x}{d\theta} - \frac{V_u}{m_u}\frac{dm_{l,u}}{d\theta} - \frac{V_b}{m_b}\frac{dm_{l,b}}{d\theta} + \frac{V_u}{T_u}\frac{dT_u}{d\theta} + \frac{V_b}{T_b}\frac{dT_b}{d\theta} - \frac{V}{P}\frac{dp}{d\theta} \tag{23}$$

Rearranging Eq. 23 to get an equation for the rate of change of the burned gas temperature:

$$\frac{dT_b}{d\theta} - \frac{P}{m_b R_b}\left[\frac{dV}{d\theta} - \left(\frac{V_b}{m_b} - \frac{V_u}{m_u}\right)\frac{dm_x}{d\theta} + \frac{V_u}{m_u}\frac{dm_{l,u}}{d\theta} + \frac{V_b}{m_b}\frac{dm_{l,b}}{d\theta}\frac{V}{P}\frac{dp}{d\theta} - \frac{V_u}{T_u}\frac{dT_u}{d\theta}\right] \tag{24}$$

Finally, substituting equations (21) and (24) in Eq. (15) result in:

$$\frac{m_u C_{v,u}}{m_u C_{p,u}}\left(V_u\frac{dp}{d\theta}-\frac{dQ_u}{d\theta}\right)$$

$$+\frac{m_b C_{v,b} p}{m_b R_b}\left[\begin{array}{c}\dfrac{dV}{d\theta}-\left(\dfrac{V_b}{m_b}-\dfrac{V_u}{m_u}\right)\dfrac{dm_x}{d\theta}+\dfrac{V_u}{m_u}\dfrac{dm_{l,u}}{d\theta}\\ +\dfrac{V_b}{m_b}\dfrac{dm_{l,b}}{d\theta}+\dfrac{V}{P}\dfrac{dp}{d\theta}-\dfrac{V_u}{m_u T_u C_{p,u}}\left(V_u\dfrac{dp}{d\theta}-\dfrac{dQ_u}{d\theta}\right)\end{array}\right]+u_b-u_u\frac{dm_x}{d\theta}$$

$$=\frac{dQ}{d\theta}-p\frac{dv}{d\theta}-R_u T_u\frac{dm_{l,u}}{d\theta}-R_b T_b\frac{dm_{l,b}}{d\theta} \qquad (25)$$

Rearranging this equation to obtain the rate of change of the cylinder pressure:

$$\frac{dp}{d\theta}=\left(\frac{C_{v,u}}{C_{p,u}}-\frac{C_{v,b}}{R_b}\frac{R_u}{C_{p,u}}V_u+\frac{C_{v,b}}{R_b}V\right)^{-1}$$

$$\left\{\begin{array}{l}-\left(1+\dfrac{C_{v,b}}{R_b}\right)p\dfrac{dV}{d\theta}-C_{p,b}T_b\dfrac{dm_{l,b}}{d\theta}\\ -\dfrac{R_u}{R_b}C_{p,b}T_u\dfrac{dm_{l,u}}{d\theta}-\dfrac{dQ}{d\theta}\\ -\left[u_b-u_u C_{v,b}\left(T_b-\dfrac{R_u}{R_b}T_u\right)\right]\dfrac{dm_x}{d\theta}\\ +\left(\dfrac{C_{v,u}}{C_{p,u}}-\dfrac{C_{v,b}}{R_b}\dfrac{R_u}{C_{p,u}}\right)\dfrac{dQ_u}{d\theta}\end{array}\right\} \qquad (26)$$

3 **Results and Discussion**

Variation of Engine Speed, Engine Load and Equivalence Ratio (Ignition Timing = 30º BTDC, Compression Ratio=10 and EGR= 0 %)

Fig. 1 to Fig. 8 shows the results for variation of equivalence ratio and engine speed at 50 % load while table 2 shows the results for variation of equivalence ratio and engine load at an engine speed of 3000 rpm. Fig. 1 shows that the lowest value for BSFC was obtained at the engine speed of 3000 rpm gives and this value increases before and after this speed. From the figure, it can be seen that BSFC increases as the equivalence ratio changes from 0.8 to 1.2. The lowest value of BSFC of 250 g/kWh was achieved at an equivalence ratio of 0.8 and engine speed of 3000 rpm while the highest value of 330 g/kWh was obtained at an engine speed of 1000 rpm and equivalence ratio of 1.2. Fig. 2 to Fig. 4 shows that engine speed of 1000 rpm gave the lowest value for BP, BMEP and thermal efficiency. The values obtained increased to a maximum at engine speed of 3000 rpm and then these values decreased when engine speed increased from 3000 rpm to 5000 rpm for different equivalence ratios considered. This result is due to the fact

that volumetric efficiency and engine friction increase with an increase in engine speed up to around 3000 rpm above which engine friction dominates. It can be seen from the figures that BP and BMEP increase as the equivalence ratio increases from 0.8 to 1.2 while thermal efficiency reduces as the equivalence ratio increases. These results agreed with the results obtained by [3,19,21] and they follow the same trend.

The highest value of BP of 33 kW was obtained at an engine speed of 3000 rpm and an equivalence ratio of 1.2 while the lowest value of 19 kW was obtained at an equivalence ratio of 0.8 and engine speed of 1000 rpm. The highest BMEP value of 1070 kPa was obtained at an equivalence ratio of 1.2 and engine speed of 3000rpm while the lowest value of 650 kPa was obtained at an equivalence ratio of 0.8 and engine speed of 1000 rpm. The highest value of 28% for thermal efficiency was obtained at an engine speed of 3000 rpm and equivalence ratio of 0.8 while the lowest value of 12% was obtained at an engine speed of 1000 rpm and equivalence ratio of 1.2.

Fig. 5 shows the effect of engine speed on exhaust gas temperature. The figure shows that exhaust gas temperature increases as engine speed increases from 1000 rpm to 5000 rpm also, exhaust gas temperature increases with an increase in the value of equivalence ratio from 0.8 to 1.2. The maximum exhaust gas temperature of 720 ^{0}C was obtained at a speed of 5000 rpm and an equivalence ratio of 1.2, while the lowest temperature of 400 ^{0}C was obtained at an engine speed of 1000 rpm and equivalence ratio of 0.8.

Fig. 6 to Fig. 8 show the results for the effects of engine speed on HC, CO and NO_X emissions at different equivalence ratio. Fig. 6 and 7 shows that HC and CO emissions are nearly constant for equivalence ratio lesser than 0.9 with a percentage increase of 2.25% and 0.96% for HC and CO emission respectively when the equivalence ratio increases from 0.8 to 0.9. The figures also show that HC and CO emissions increase sharply for equivalence ratio greater than 0.9 with a percentage increase of 23.46% and 37.14% for HC and CO emissions respectively when the equivalence ratio increases from 0.9 to 1.0. It can be seen that HC and CO emissions increase moderately with increasing speed from 1000 rpm to 5000 rpm.

The highest HC Emission of 2700 ppm was obtained at an engine speed of 5000 rpm and equivalence ratio of 1.2 while the lowest emission of 1400 ppm was obtained at an engine speed of 1000 rpm and equivalence ratio of 0.8. For CO emission, the highest value of 9600 ppm was obtained at a speed of 5000 rpm and equivalence ratio of 1.2 while the lowest emission of 4800 ppm was obtained at an engine speed of 1000 rpm and equivalence ratio of 0.8. Fig. 8 shows that

the engine speed of 3000 rpm gives the highest value for NO_X emission and this value reduces before or after this speed. The figure also shows that NO_X emission increases sharply from the equivalence ratio of 0.8 until the emission peaked at an equivalence ratio of 0.9 before it reduces when the equivalence ratio increases from 0.9 to 1.2. The maximum NO_X emission is obtained at an engine speed of 3000 rpm and equivalence ratio of 0.9 while the lowest emission is obtained at an engine speed of 1000 rpm and equivalence ratio of 1.2.

Table 2 shows the effect of equivalence ratio and engine load on the performance characteristics of the SI engine at a constant engine speed of 3000 rpm. The results show that thermal efficiency decreases with an increase in engine load while the other parameters increase with an increase in engine load at all the equivalence ratios considered. It can also be seen from the table that NO_X emission peaked at an equivalence ratio of 0.9 and an engine load of 100%. The results obtained in this work are agreement with the results obtained by [2,3,5, 19] and they follow the same trend.

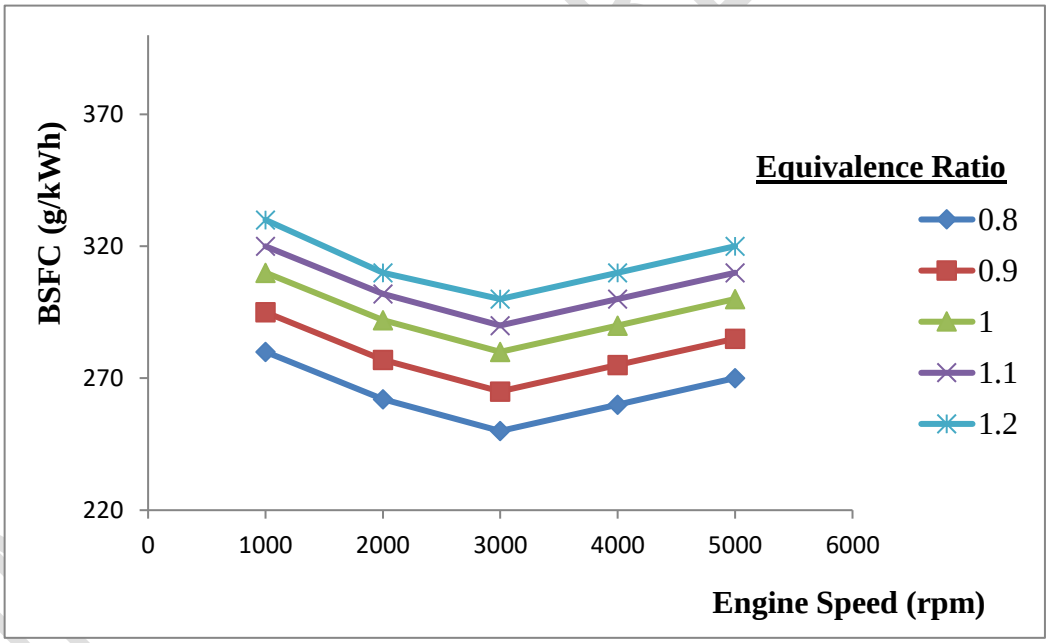

Figure 1: Effect of Engine Speed on BSFC at Different Equivalence Ratio

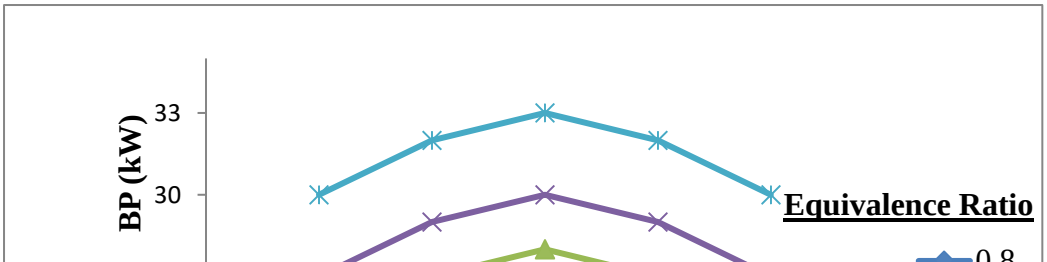

Figure 2: Effect of Engine Speed on Brake Power at Different Equivalence Ratio

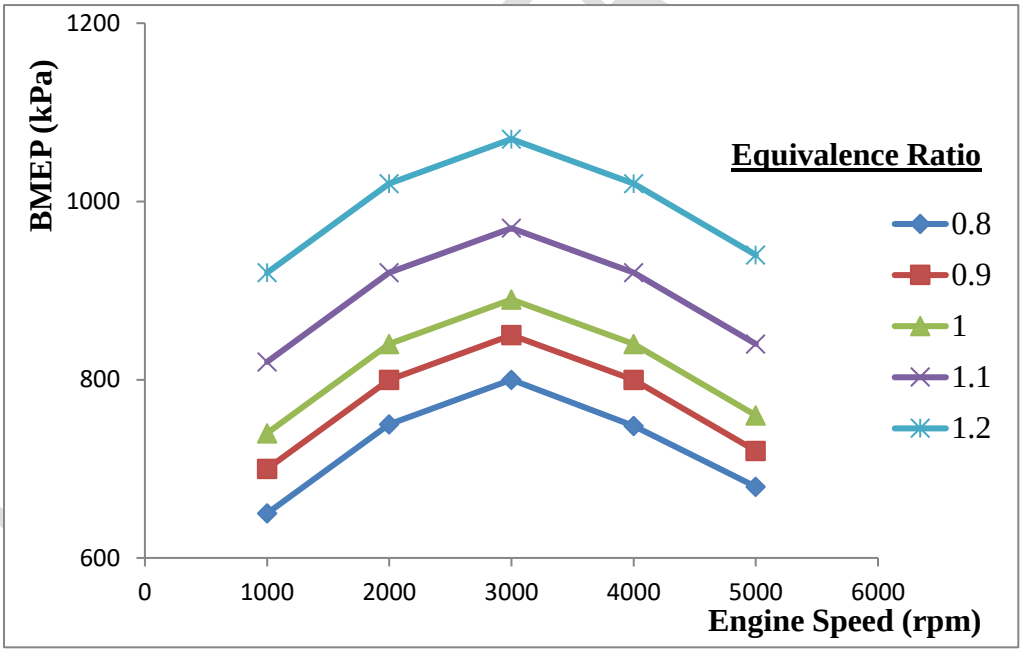

Figure 3: Effect of Engine Speed on BMEP at Different Equivalence Ratio

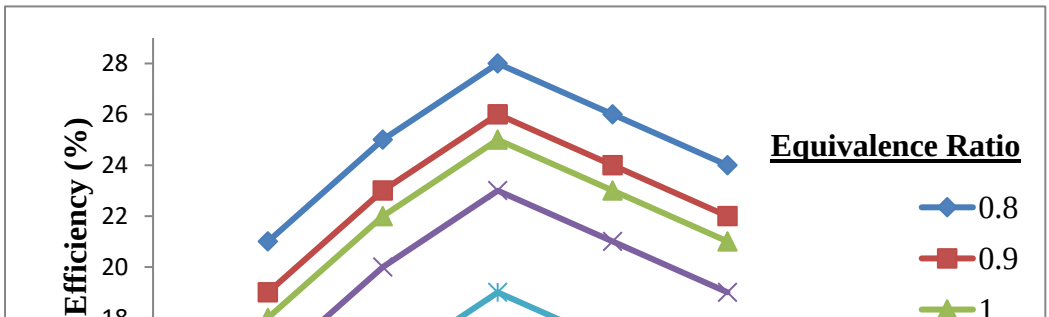

Figure 4 : Effect of Engine Speed on Thermal Efficiency at Different Equivalence Ratio

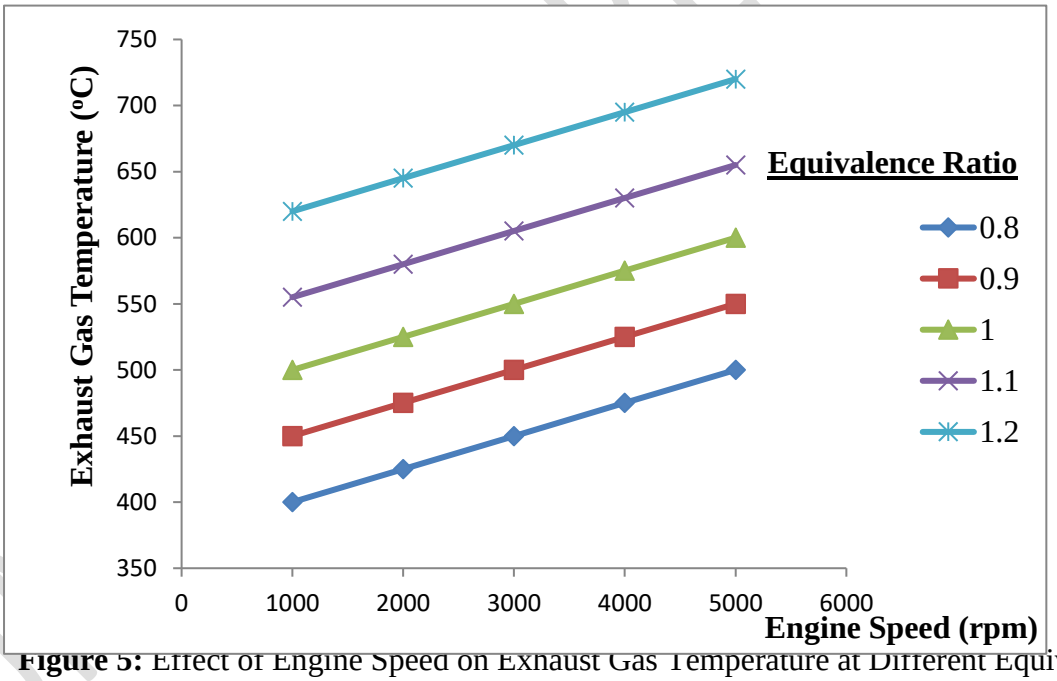

Figure 5: Effect of Engine Speed on Exhaust Gas Temperature at Different Equivalence Ratio

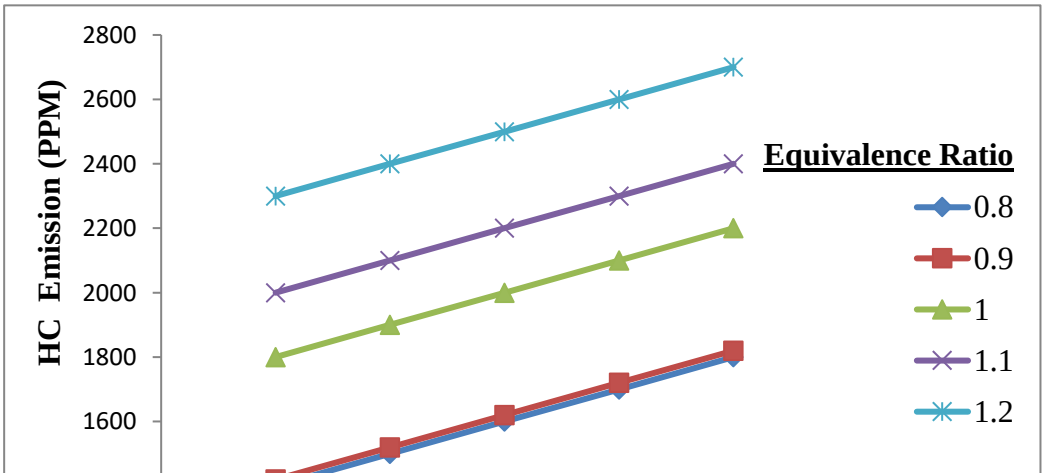

Figure 6: Effect of Engine Speed on HC Emission at Different Equivalence Ratio

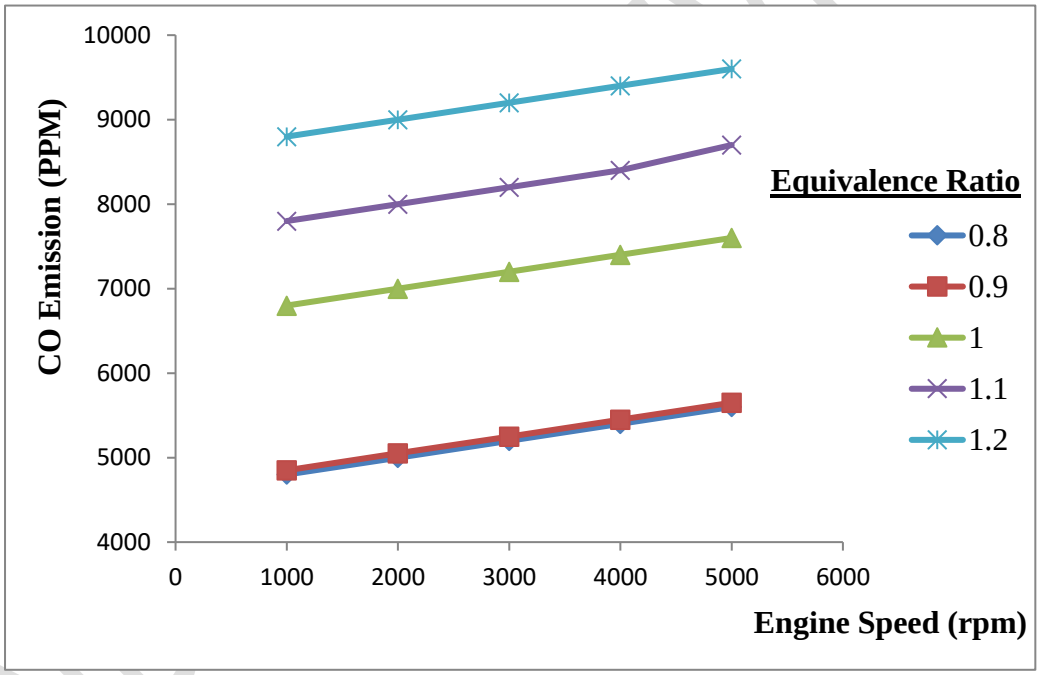

Figure 7: Effect of Engine Speed on CO Emission at Different Equivalence Ratio

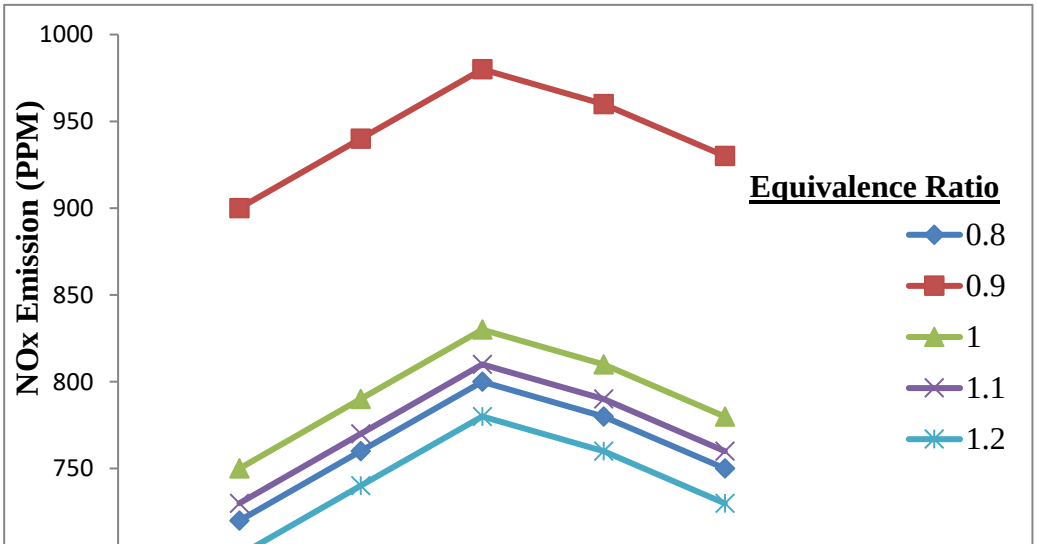

Figure 8: Effect of Engine Speed on NO_X Emission at Different Equivalence Ratio

Table 2: Effect of Equivalent Ratio and Engine Load on Performance Characteristics of SI Engine

S/N	Engine Load (%)	Equivalence Ratio	BSFC (g/kWh)	BP (kW)	BMEP (kPa)	η_{TH} (%)	T_{EG} (^oC)	HC (PPM)	CO (PPM)	NO_X (PPM)
1	0	0.8	210	15	320	28	380	1200	4600	550
2	25	0.8	225	16	420	27	410	1350	4850	600
3	50	0.8	240	17	490	26	440	1500	5100	650
4	75	0.8	255	18	580	25	470	1650	5350	700
5	100	0.8	270	19	670	24	500	1800	5600	750
6	0	0.9	225	18	370	26	430	1220	4650	730
7	25	0.9	240	19	420	25	460	1370	4900	780
8	50	0.9	255	20	540	24	490	1520	5150	830
9	75	0.9	270	21	630	23	520	1670	5400	880
10	100	0.9	285	22	720	22	550	1820	5650	930
11	0	1.0	240	21	410	25	480	1600	6600	580
12	25	1.0	255	22	510	24	510	1750	6850	630
13	50	1.0	270	23	580	23	540	1900	7100	680
14	75	1.0	285	24	670	22	570	2050	7350	730
15	100	1.0	300	25	760	21	600	2200	7600	780
16	0	1.1	250	23	490	23	535	1800	7600	560
17	25	1.1	265	24	590	22	565	1950	7850	610
18	50	1.1	280	25	660	21	595	2100	8100	660
19	75	1.1	295	26	750	20	625	2250	8350	710
20	100	1.1	310	27	840	19	655	2400	8700	760
21	0	1.2	260	26	590	19	600	2100	8600	530
22	25	1.2	275	27	690	18	630	2250	8850	580
23	50	1.2	290	29	760	17	660	2400	9100	630
24	75	1.2	305	29	850	16	690	2550	9350	680
25	100	1.2	320	30	940	19	720	2700	9600	730

4 Conclusions

The theoretical analysis of performance parameters of a non-road SI engine has been carried out in this research. The analysis was done to investigate the effects of three operating parameters of SI engines on performances characteristics of non-road SI engines. This study showed that an engine speed of about 3000 rpm gave the optimum values for all the parameters considered and that the values of these parameters increased as the value of the engine load increased. An equivalence ratio of about 0.9 gave the optimum values for all the parameters

considered. It can be deduced from this research that for lower brake specific fuel consumption, optimum engine efficiency and lower exhaust gas emissions then, the non-road SI engine should be operated at low engine loads, engine speed of about 300 rpm and an equivalence ratio of 0.9. It is therefore concluded that the two-zone SI engine model used and computer code developed is adequate and robust enough to predict the performance characteristics of a non-road SI engine.

List of Abbreviations

SI	Spark Ignition
HC	Hydrocarbon
CO	Carbon monoxide
NO_x	Oxides of Nitrogen
BSFC	Brake Specific Fuel Consumption
BP	Brake Power
BMEP	Brake Mean Effective Pressure
EGR	Exhaust Gas Recirculation

Declarations

Availability of data and material

The datasets used or analyzed during the current study are available from the corresponding author on reasonable request.

Disclaimer (Artificial intelligence)

Author(s) hereby declare that NO generative AI technologies such as Large Language Models (ChatGPT, COPILOT, etc.) and text-to-image generators have been used during the writing or editing of this manuscript.

5 References

[1] National Bureau of Statistics (NBS). (2021). *Nigeria Gross Domestic Product Report, Q1 2021*. Retrieved from https://nigerianstat.gov.ng

[2] Onawunmi A.S., Fayomi O.S.I, Okolie S.T.A., Adio T.A., Udoye N.E. Samuel A.U. (2019). Determination of a Spark-Ignition Engine's performance parameters using Response Surface Methodology. *Energy Procedia*. Vol. 157. Pp. 1412 -1422

[3] Heywood J.B. (2018): Internal combustion engine fundamentals (2nd edition). *MC Grow-Hill education New York.* Pp. 999.

[4] An Y., Tang W., Vallinayagam R., Shi H., Sim J., Chang J. Magnotti G. and Johansson B. (2019): Combustion stability study of partially premixed combustion by High-pressure multiple injections with Low-Octane fuel. *Applied Energy*. Vol. 248 pp. 626-639.

[5] Esposito S., Cai L., Gunther M., Pitsch H. and Pischinger S. (2020): Experimental Comparison of combustion and emission characteristics between a market gasoline and its surrogate. *Combustion and flame*. 214 Pp. 306 – 322.

[6] Andwari A.M., Pesyridis A., Esfahanian V. and Said M.F.M. (2019): Combustion and emission enhancement of a spark-ignition two-stroke cycle engine utilizing internal and external exhaust gas recirculation approach at low-load operation. *Energies* 12. Pp. 609 – 625.

[7] Delvi H.A., Faheem M., Khan S.A., Kumar K.M. and Kareemullah M. (2019): Effect of Ethanol-Gasoline blends on performance, combustion and emission characteristics of a spark-ignition engine. Journal of advanced research in fluid mechanics and thermal sciences. Vol. 62 (2) Pp. 209 – 220.

[8] Mohiuddin k, Kwon H, Chio M and Park S. (2021). Effect of engine compression ratio, injection timing and exhaust gas recirculation on gaseous and particle number emissions in a light-duty diesel engine. *Fuel.* 294 Pp. 52-70

[9] Kaplan M., Ozbey M. and Ozcan H. (2018): Numerical investigation of the effects of intake port geometry on In-cylinder motion and combustion in a diesel engine. *The international journal of engineering and science*. **7** (6). Pp. 16-26.

[10] National Environmental Standards and Regulations Enforcement Agency (NESREA). (2018). *National Environmental (Air Quality Control) Regulations, S. I. No. 62 of 2018*. Retrieved from http://nesrea.gov.ng

[11] U.S. Environmental Protection Agency (EPA). (2020). Nonroad Engines, Equipment, and Vehicles: Emission Standards Reference Guide. Retrieved from https://www.epa.gov

[12] Akbiyik T, Kahiaman N, and Tanep T. (2023). Energy and Exergy Analysis with Emissions Evaluation of a Gasoline Engine using different fuels. Fuel 345-364

[13] Biswal A., Kale R., Teja G.R., Baneejee S., Kolhe P and Balusanly S. (2020). An Experimental and Kinetic Modeling Study of Gasoline/Lemon Peel Oil Blends for PFI Engine. *Fuel* **267**, 367-378.

[14] Costa J; Martins J; Arantes T; Goncalves M; Durao L; and Brito F. P. (2021). Experimental Assessment of the Performance and Emissions of a Spark-Ignition Engine Using Waste-Derived Biofuels as Additives. *Energies* 14(16), 106 – 114.

[15] Elshenawy, M. A., Abou El-Maaty, M. A., El-Gohary, M. H., and El-Sayed, M. A. (2023). Recent Advances in Fuel Blends for Internal Combustion Engines: A Review of Performance, Emissions, and Future Directions. *Energy Reports*, 9, 252-275.

[16] Ahmed E; Usman M; Anwar S; Ahmad H. M; Nasir M.W. and Malik M.A. (2021). Application of ANN to Predict Performance and Emissions of SI Engine Using Gasoline-Methanol Blends. *Science Progress* 104(1), 1 – 27.

[17] Iliev, I., Borojevic, D., and Jovanovic, M. (2021). Performance and Emissions of Internal Combustion Engines Fueled by Alternative Fuels: A Review. *Energy Reports*, 7, 332-354

[18] Jiahong F; Ruomiao Y; Xin L; Xiaoxia S; Yong L; Zhentao L; Yu Z. and Bengt S. (2022). Application of Artificial Neural Network to Forecast Engine Performance and Emissions of a Spark Ignition Engine. *Applied Thermal Engineering*. 201, 411 – 424.

[19] Lius, Lin Z, Zhang H, Fan Q, Lei N, and Wang Z (2023). Experimental Study on Combustion and Emission Characteristics of Ethanol- Gasoline Blends in a High Compression Ratio SI Engine. Energy. D01:10.1016/ j. *Energy 2023*. 127398.

[20] Zhang Y; Wang Q; Chen X; Yan Y; Yang R; Lie Z. and Fu J. (2022). The Prediction of Spark-Ignition Engine Performance and Emissions Based on the SVR Algorithm. *Processes* 10, 201 – 221.

[21] Karagoz Y; Balci O; Gezer O; Koten H; and Isin O. (2021). Performance and Emissions of Spark–Ignition Engines Fuelled with Petrol and Methane. *Proceeding of the Institution of Civil Engineers.* Energy. 174(4), 156 – 169.